

The composition dependence of the Raman spectrum and new assignment of the phonons in  
**LiNbO<sub>3</sub>**

This article has been downloaded from IOPscience. Please scroll down to see the full text article.

1997 J. Phys.: Condens. Matter 9 9687

(<http://iopscience.iop.org/0953-8984/9/44/022>)

View [the table of contents for this issue](#), or go to the [journal homepage](#) for more

Download details:

IP Address: 171.66.16.209

The article was downloaded on 14/05/2010 at 10:58

Please note that [terms and conditions apply](#).

# The composition dependence of the Raman spectrum and new assignment of the phonons in $\text{LiNbO}_3$

A Ridah†, P Bourson‡, M D Fontana and G Malovichko§

Laboratoire Matériaux Optiques à Propriétés Spécifiques, CLOES—University of Metz and Supelec, 2 rue E Belin, 57078 Metz Cédex 3, France

Received 4 March 1997, in final form 30 May 1997

**Abstract.** The Raman spectrum of  $\text{LiNbO}_3$  has been measured for various scattering configurations in crystals with different compositions. The comparison between spectra recorded for the congruent and the nearly stoichiometric crystals shows significant differences in the shape and the number of Raman peaks. The analysis of results leads to a new and complete assignment of the long-wavelength optical phonons in  $\text{LiNbO}_3$ .

## 1. Introduction

The lattice dynamics of  $\text{LiNbO}_3$  (LN) has been the object of numerous investigations using the Raman [1–3] and the IR reflectivity [4] spectroscopy. Despite this, the phonon characteristics were not clearly established and some disagreements have been reported between various authors [2, 3]. All these investigations were carried out on crystals with the congruent composition, in which the Li deficit is nearly 3% with respect to the stoichiometric composition. Recently, the possibility of obtaining crystals with off-congruent compositions was shown using vapour transport equilibration techniques [5] or by introducing  $\text{K}_2\text{O}$  in the melt [6]. It was then proved that several properties of LN, such as the optical absorption edge and the refractive indices, are dependent on the concentration of the non-stoichiometry defects in the crystal [6, 7]. The possible variation of the Raman lines (shape and positions) with the composition or the Li/Nb concentration ratio in the crystal has not until now been investigated. However the Raman scattering technique is one of several methods which could be used to determine the composition from the measurement of the width of some particular lines [8].

The goal of our paper is to revise the assignment of optical phonons and to attempt to remove some ambiguities earlier reported thanks to the new measurements in off-congruent crystals. For this, we decided to study the influence of the crystal composition on the whole Raman spectrum recorded in several geometrical configurations. The comparison of the Raman data obtained for the congruent and the nearly stoichiometric crystals reveals some differences which lead us to propose a new assignment of the long-wavelength optical phonons.

† Permanent address: Laboratoire de Physique du Solide, Faculté des Sciences Ben M'Sick, Université Hassan II, Mohamedia, Casablanca, Morocco.

‡ E-mail address: bourson@esemetz.ese-metz.fr

§ Permanent address: Institute for Materials Sciences, Krjijanosvkogo 3, 252180 Kiev, Ukraine.

A complete and clear assignment can thus provide some useful information to understand the nature of the phase transitions and the origin of some physical and optical properties of lithium niobate [2].

## 2. Experimental details

LN crystals have been grown by the Czochralski technique with various initial compositions of  $\text{Li}_2\text{O}$  and  $\text{Nb}_2\text{O}_5$  in the melt:  $R_m = [\text{Li}]/[\text{Nb}] = 0.9457$  and  $R_m = 1.2$ .

At room temperature, the LN crystal belongs to the  $R3c$  space group with two molecules per unit cell. Accordingly, 18 vibrational modes at zero wavevector are decomposed into  $4A + 9E + 5A_2$ . Whereas the  $A_2$  phonons are Raman inactive,  $A_1$  and  $E$  modes are both Raman and infrared active.  $A_1$  modes are polarized along the  $Z$  axis while the doubly degenerate  $E$  modes correspond to ionic motions along  $X$  or the  $Y$  axis. Hereafter we consider the co-ordinate  $XYZ$  system where  $X$  refers to the crystallographic axis  $a$ ,  $Z$  is along the ferroelectric  $c$  axis and  $Y$  is normal to  $X$  and  $Z$ .

Raman scattering experiments have been performed in right-angle geometry using a Spex double monochromator and a 5145 Å exciting line of an Ar-ion laser with 200 mW output power.

Among other techniques [6], the exact composition  $x_c = [\text{Li}]/([\text{Li}] + [\text{Nb}])$  of the LN crystal can be found from the linewidth of some Raman lines, as shown by Schlarb *et al* [8]. The composition of our samples has been determined from linewidth  $\Gamma$  for the lowest-frequency  $E(\text{TO}_1)$  peak which is very intense and well separated from other lines.

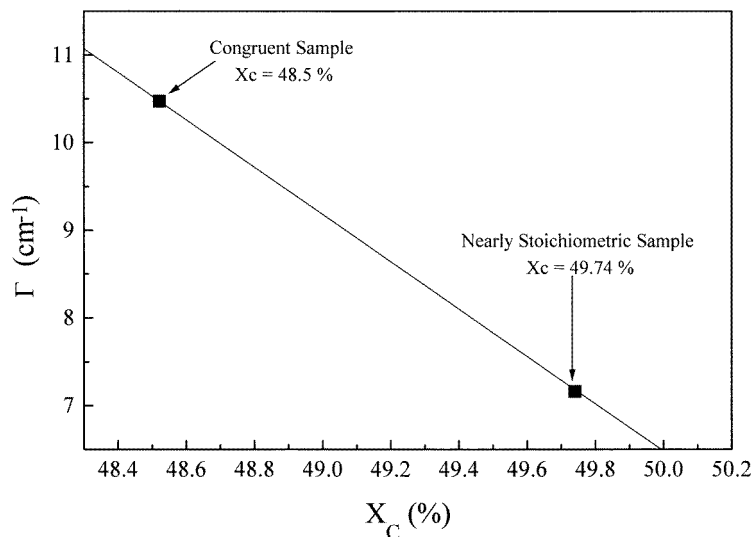


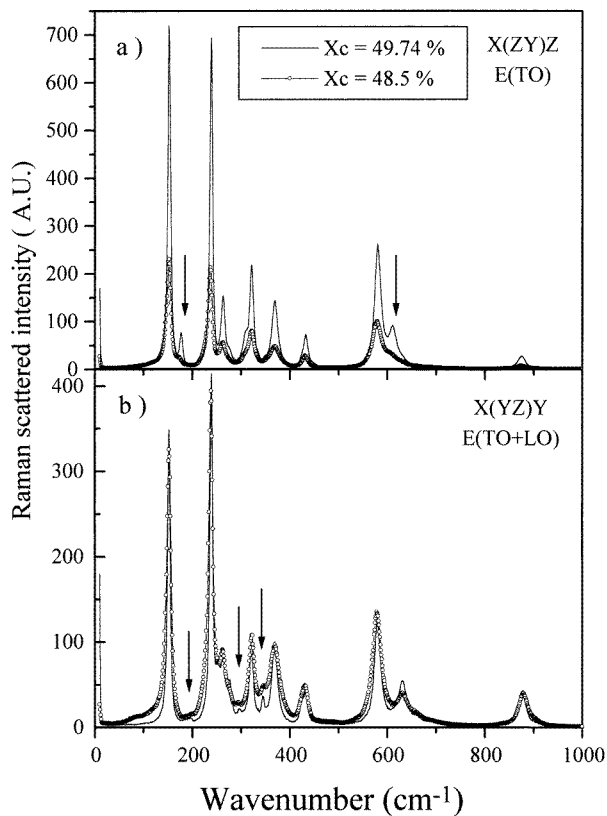
**Figure 1.** Dependence of the  $E(\text{TO}_1)$  Raman linewidth on the crystal composition  $x_c = [\text{Li}]/([\text{Li}] + [\text{Nb}])$ .  $x_c = 50\%$  corresponds to a exact stoichiometric composition. The straight line results from a calibration with standard crystals. The compositions of the samples used in our Raman investigation are deduced from this plot.

The plot  $\Gamma(x_c)$  reported in figure 1 has been established from studies on several standard materials for which composition was given by other techniques such as the phase matching temperature and the absorption edge [9]. We have found the values  $x_{c1} = 48.5\%$  and

$x_{c2} = 49.74\%$  for our samples, which are hereafter called the congruent crystal and the nearly stoichiometric crystal respectively.

### 3. Results

We have measured both  $A_1$  and E modes but we particularly pay attention to the E phonons since some discrepancies were reported for this symmetry. Purely transverse E(TO) modes can be detected in the  $X(ZY)Z$  configuration whereas E(TO) and E(LO) phonons are simultaneously detected in the  $X(YZ)Y$  or  $X(ZX)Y$  geometry. According to the group theory, nine and 18 Raman lines are respectively expected.



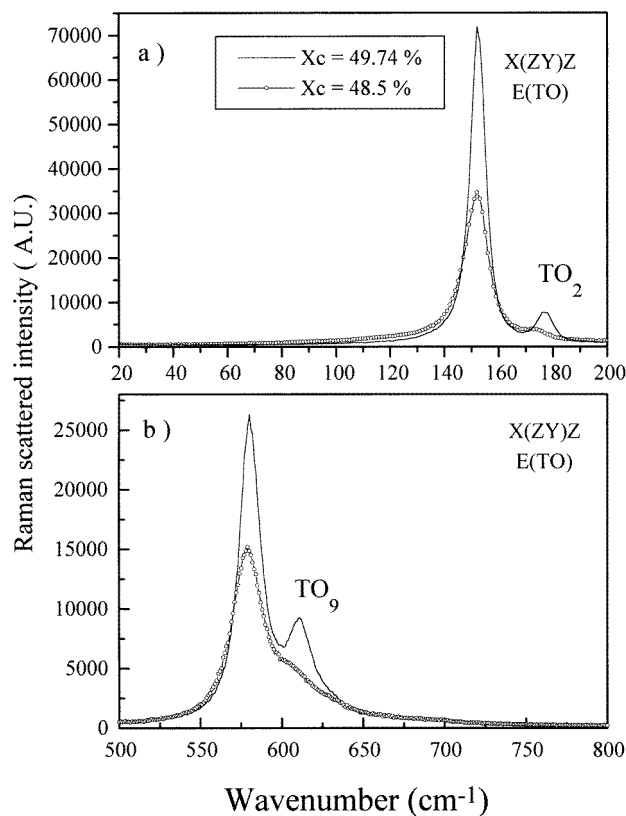
**Figure 2.** Raman spectra recorded for the LN crystals with compositions  $x_c = 49.7\%$  and  $x_c = 48.5\%$ . The arrows point the frequency ranges where new lines clearly appear for the nearly stoichiometric crystal.

Figure 2 exhibits the Raman spectra recorded in the two geometries for both samples. First, we note that the lines are thinner, better resolved and more intense for the nearly stoichiometric sample compared with the congruent sample. Therefore, first-order phonons can be unambiguously attributed only to peaks which clearly appear in the spectrum for the stoichiometric sample. Thus, in the E(TO) spectrum, one peak is detected just below  $200\text{ cm}^{-1}$  and another one just above  $600\text{ cm}^{-1}$  for the stoichiometric crystal, instead of weak shoulders of intense peaks in the case of the spectrum recorded for the congruent

sample. In the E(TO) + E(LO) spectrum (see figure 2(b)), well defined lines occur around 200, 300 and 350  $\text{cm}^{-1}$  for the nearly stoichiometric crystal. These lines are hidden by an intense and continuous background in the corresponding spectrum recorded for the congruent sample.

Moreover, this last spectrum exhibits bands at low frequency (below 100  $\text{cm}^{-1}$ ) and above 660  $\text{cm}^{-1}$  which are absent in the spectrum for the nearly stoichiometric sample.

The new lines appearing in the E(TO) spectrum for the stoichiometric sample are more clearly seen in figure 3. Thus, peaks at 177 and at 610  $\text{cm}^{-1}$  are unambiguously assigned and attributed to E(TO<sub>2</sub>) and E(TO<sub>9</sub>) phonons. It is also clear that no line exists beyond 650  $\text{cm}^{-1}$  in the E(TO) spectrum contrary to what was previously reported [1, 3]. The X(ZY)Z spectrum (see figure 2(a)) exhibits all in all nine well resolved lines which correspond to all E(TO) phonons which are expected by the crystal symmetry. Their frequencies and dampings are reported in table 1. E(LO) lines are also properly assigned by the comparison between the X(ZY)Z and X(YZ)Y spectra and reported in table 1.



**Figure 3.** Comparison of the Raman spectra recorded for LN crystals with two different compositions to point out the existence of new E(TO) lines.

Figure 4 exhibits the spectrum recorded in the X(ZZ)Y configuration corresponding to the detection of pure A<sub>1</sub>(TO) phonons. As expected by group theory, four peaks were detected around 252, 276, 333 and 633  $\text{cm}^{-1}$ . These positions are very close to those previously reported [2, 3]. However, additional bands with weak scattered intensities

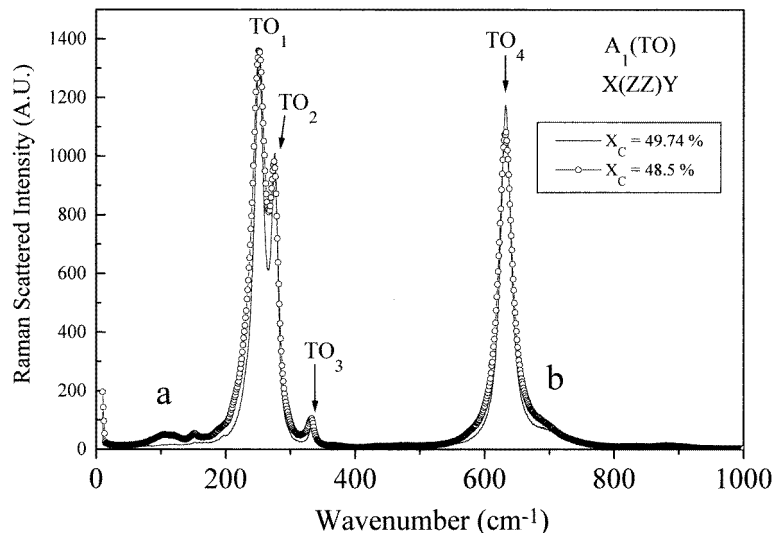


Figure 4.  $A_1(\text{TO})$  Raman spectra recorded in LN crystals with two compositions.

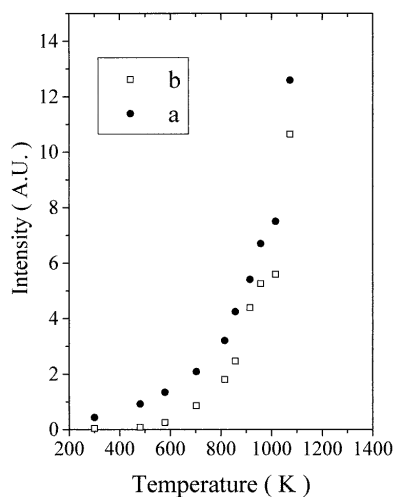


Figure 5. Temperature dependence of the scattered Raman intensity for the bands a and b.

labelled a and b were observed around  $700$  and  $100\text{ cm}^{-1}$ . Their intensities are relatively enhanced when we proceed from the stoichiometric to the congruent crystal. In fact, it can be shown that these bands probably arise from two-phonon density of states. As reported in figure 5 their intensity displays a temperature dependence similar to the intensity behaviour characteristic of second-order processes (a complete Raman study as a function of the temperature was recently reported in [10]). The bands a and b are also seen in the E spectra specially for the congruent sample (see figure 2(b)). This means that their intensity is enhanced in both E and  $A_1$  spectra with increasing number of non-stoichiometric intrinsic defects and/or with increasing temperature. Therefore, they are probably due to a breaking of

**Table 1.** E(TO) and E(LO) phonon characteristics obtained in our Raman investigation. Frequencies and dampings (in brackets) are deduced from the fit of the Raman lines to damped oscillators. These results are compared with the previous Raman data reported by Kaminow and Johnston [2] and Claus *et al* [3] and with the infrared results given by Servoin [4]. New phonons which are first evidenced in the nearly stoichiometric crystal are pointed out by boxes, while the stars indicate the peaks which were erroneously attributed to the first-order phonons in previous investigations.

Servoin Infrared		Kaminow and Johnston Raman		Claus <i>et al</i> Raman		Our work Raman	
E(TO)	E(LO)	E(TO)	E(LO)	E(TO)	E(LO)	E(TO)	E(LO)
		92*	117*				
150	176	152	198	155	198	152.8 (7.8)	186.5 (11.8)
177	195					<u>177.3 (9.3)</u>	194.9 (17.2)
228*	238	238	243	238	243	238.3 (7.5)	240.4 (5.3)
262	279*	262	298	265	295	264.2 (5.3)	299.0 (15)
282*	295						
322	344	322	345	325	371*	321.9 (13.9)	<u>345.0 (10.0)</u>
362	425			371	428	369.5 (19.5)	424.2 (7.6)
434	456	436	448	431	454	432.4 (13.0)	456.0 (28.6)
580	881	582	621	582	668*	580.0 (17.8)	<u>625 (18.6)</u>
		630*	881	668*	739*		
				743*	880	<u>609.8 (30.5)</u>	878 (21.6)

the Raman selection rules due to the presence of intrinsic defects in the congruent crystal, leading to the detection of broad density of states bands. These bands have often been erroneously attributed in the literature to normal first-order phonon scattering [2].

#### 4. Discussion

Now we turn to the comparison with the results reported in the literature and we particularly point out the differences and the new attributions.

We focus our attention on the E phonons, which are the main object of disagreements in the literature. As shown in table 1, significant discrepancies are found if we compared our results with previous infrared and Raman data.

First Raman measurements were reported by Schaufele and Weber [1]. Instead of nine expected lines only seven lines were assigned to the E(TO) phonons. More complete studies were performed by Kaminow and Johnston [2] and Claus *et al* [3]. Some discrepancies have been already noted between these two results [3]. The main difference arises from the attribution of the low-frequency band around  $90\text{ cm}^{-1}$ , which was detected in both investigations. We have clearly shown above that this band disappears (see figure 2) when the crystal composition is close to stoichiometry. This proves that this band has no intrinsic origin and has to be unambiguously discarded in the assignment.

Compared with the study of Claus *et al* [3], we exclude a first-order origin of the broad bands lying above  $650\text{ cm}^{-1}$  in our new assignment. These bands were observed in various previous investigations which all were performed for congruent samples. It is clearly shown in figures 2 and 3 that the intensities of these bands decrease with a lowering of the intrinsic defect concentration.

Instead of these bands, we consider that the well resolved lines around 177 and  $610\text{ cm}^{-1}$  can be clearly attributed to first-order E(TO) phonons.

In this paper, we have compared Raman results obtained in pure lithium niobate for two

different compositions. Our data obtained in the congruent crystal are quite similar to those previously reported [2, 3]. The new assignment of the lattice modes in  $\text{LiNbO}_3$  reported here was rendered possible thanks to the recent availabilities of more perfect samples. The difference between Raman spectra recorded in congruent and nearly stoichiometric crystals only concerns the less intense peaks. In the stoichiometric sample well resolved lines appear instead of wide bands detected in the congruent sample. These bands therefore arise from the activation by intrinsic defects of the phonons belonging to the whole Brillouin zone. Other broad bands appearing in the congruent sample only, and previously assigned in the literature as first order phonon lines, are here attributed to two-phonon density of states. On the other hand, some new lines occur only in the nearly stoichiometric crystal, so we obtain a new and complete description of the long-wavelength optical phonons.

### Acknowledgment

We are very grateful to K Polgar, who kindly supplied the crystals used for calibration of the plot  $\Gamma(x_c)$ .

### References

- [1] Schaufele R F and Weber M J 1966 *Phys. Rev.* **152** 705
- [2] Kaminow I P and Johnston W D 1967 *Phys. Rev.* **160** 519
- [3] Claus R, Borstel G, Wiesendanger E and Steffan L 1972 *Z. Naturf. a* **27** 1187
- [4] Servoin J L 1980 *Thesis* Orléans  
Servoin J L and Gervais F 1979 *Solid State Commun.* **31** 387
- [5] Bordui P F, Norwood R G, Jundt D H and Feyer M M 1992 *J. Appl. Phys.* **71** 875
- [6] Malovichko G I, Grachev V G, Kokanyan P, Schirmer O F, Betzler K, Gather B, Jermann F, Klauer S, Schlarb U and Wöhlecke M 1993 *Appl. Phys. A* **56** 103
- [7] Schirmer O F, Thiemann O and Wöhlecke M 1991 *J. Phys. Chem. Solids* **52** 185
- [8] Schlarb U, Klauer S, Wesselmann M, Betzler K and Wöhlecke M 1993 *Appl. Phys. A* **56** 311
- [9] Földvari I, Polgar K, Voszka R and Balasanyan R N 1984 *Cryst. Res. Technol.* **19** 1659
- [10] Ridah A, Fontana M D and Bourson P *Phys. Rev. B* **56** 5967